Eur Food Res Technol (2008) 226:1545–1552
DOI 10.1007/s00217-007-0685-x

ORIGINAL PAPER

Effect of sun-drying on microstructure and texture of S. Bartolomeu pears (*Pyrus communis* L.)

Dulcineia Ferreira · José A. Lopes da Silva · Glória Pinto · Conceição Santos · Ivonne Delgadillo · Manuel A. Coimbra

Received: 2 March 2007 / Revised: 20 May 2007 / Accepted: 28 May 2007 / Published online: 26 June 2007
© Springer-Verlag 2007

Abstract Histological and mechanical studies were conducted to evaluate the changes that are conferred by a traditional sun-drying process on the texture and microstructure of a Portuguese pear cultivar (*Pyrus communis* L. var. S. Bartolomeu). Sun-drying processing of the pears results in loss of water, cell flattening and shrinkage, loss of cellular adhesion, and even loss of cell wall integrity. The sun-drying process significantly reduced the hardness and fracturability of the pear tissues, while increasing their cohesiveness, springiness and adhesiveness. The results obtained by texture and microstructure analysis of the fresh pear flesh reflect essentially an unified matrix comprising well-packed cells strongly bonded together whereas those of the sun-dried pear flesh pointed out a soft solid with many individual cells distributed in a soft matrix, explaining its softer and chewy texture.

Keywords Pears · Sun-drying · Microstructure · Scanning electron microscopy · Texture profile analysis

D. Ferreira · J. A. L. d. Silva · I. Delgadillo · M. A. Coimbra (✉)
Departamento de Química,
Universidade de Aveiro, 3810-193 Aveiro, Portugal
e-mail: mac@dq.ua.pt

G. Pinto · C. Santos
CESAM, Departamento de Biologia,
Universidade de Aveiro, 3810-193 Aveiro, Portugal

D. Ferreira
Escola Agrária de Viseu, Instituto Politécnico,
Quinta da Alagoa, Estrada de Nelas,
3500-606 Viseu, Portugal

Introduction

Drying of fruits and vegetables is one of the oldest forms of food preservation. Although the sun-drying process has lost its importance giving in to newer technologies, it is still practised in many places around the world as an effective means of food preservation [1, 2].

In Portugal, the sun-drying process is used for the home-made small-scale processing of S. Bartolomeu pear, especially by smallholders. Despite the cheap and environmental friendly characteristics of the solar drying process, there is still a lack of knowledge on the traditional sun-drying practice to allow better process control and reproducibility of product characteristics, in a proper way to ensure a high quality product and to minimise post-harvest losses. The sun-dried pear is a regional Portuguese food product with distinctive texture, taste, colour, and favour organoleptic characteristics. The sun-dried pears of the local variety known as S. Bartolomeu are relatively small fruits, characterised by an intense reddish brown colour containing a large number of stone cells and pronounced astringency. With drying [3], the astringency is lost and the fruit achieves a typical sweet flavour and chewy texture.

Drying is a complex process whose mechanisms are not yet entirely understood. Complex biological and chemical reactions occur during the drying process and they will greatly influence microstructure and texture of the vegetable tissues. Typically, the reduction of the moisture content to a level, which allows safe storage over an extended period, also causes shrinkage of the fruit. Loss of water and cell wall integrity can originate flaccid tissues with a rubber texture [4]. Hills and Remigereau [5], while studying the air-drying of parenchyma apple tissues, have shown that water loss occurs mainly from the vacuole compartment,

whereas minor changes in water content occur in the cytoplasm or in the cell wall compartments. The shrinkage of tissues is related to loss of turgor pressure and to decline of cell wall integrity, thus causing important textural changes that will play an important role in the quality of the dried product.

Texture is the result of complex interactions among food components, spanning the molecular, supramolecular and the microstructural levels [6]. Consumer acceptability of fruits and vegetable commodities is of utmost importance. There has been great interest in the development of methods to predict and control the texture of plant-based foods, particularly in relation to processing and/or post-harvest treatments. This requires the knowledge on mechanical properties of cellular materials, microstructure, and the chemistry and biochemistry of the cell wall. The cell wall and the middle lamella are known to control the way in which vegetable tissues undergo mechanical deformation and failure during mastication [7]. The correlation between instrumental measurements of rheological and textural properties and the subjective sensorial product evaluation has also been the subject of many research efforts [8].

The changes in texture occurring during the processing of plant materials or certain physiological events have been related to tissue and cell microstructural changes, namely to the integrity loss of cell wall and middle lamella, changes on cell adhesion, structural changes on pectic fractions, and to increasing solubility of the cell wall polysaccharides [7, 9–14]. Similar structural changes on cell wall polysaccharides during sun-drying have also been reported for pears [15] and other fruits [16, 17].

Changes on cell wall polysaccharides [15] and on phenolic compounds [18] during the sun-drying process of S. Bartolomeu pears have been previously reported. Texture attributes of plant materials are known to be related to histological factors, such as the size and shape of the cells, cell adhesion and intercellular spaces, cell wall properties and the cell turgor pressure [19–21]. In this work we evaluated the microstructural and textural changes that occurred due to traditional sun-drying of S. Bartolomeu pears. A better fundamental understanding of the biochemical and microstructural changes occurring during the sun-drying process, and how these changes are related to texture variation, is expected to lead ultimately to a better process control, and final product quality, valorisation, and acceptance.

Materials and methods

Pear samples

The analyses were performed on a single lot of fresh and sun-dried peeled pears (*Pyrus communis* L. var. S. Bartolomeu). Both lots were obtained from the same producer, located at village of S. Gião, Oliveira do Hospital, Portugal, geographically localised at 40.3330° N, and 7.8000° W in 704 m of altitude, and harvested at the commercial maturity stage.

Harvesting and processing occurred during July/August. After harvesting, the pears were peeled and allowed to sun-dry for nearly 5 days. Then the pears were laid in baskets and covered with a cloth during 2 days. This treatment is necessary for equalisation of moisture content in the internal and external parts of material, which prevents material fracture and gives the pears the elasticity needed to flatten without breakage. The flattening consists in a compression of each pear on the two sides with a specific instrument. With this procedure the pears acquire a thickness of 10 mm, on maximum. After this, the pears are submitted to a second sun-drying process. The final product is a small dried pear with a reddish-brown colour and peculiar elastic properties.

The average moisture content of fresh and sun-dried pears was $85 \pm 2\%$ and $20.6 \pm 0.1\%$, respectively. The average weight of fruit was 58 ± 13 g for fresh pears and 10 ± 2 g for sun-dried pears.

Scanning electron microscopy (SEM)

Material preparation and fixation for SEM analysis were performed as previously described [22]. Briefly, the parenchyma tissue was cut into 2×4 mm slices, on the transversal line in different regions of pear mesocarp, and fixed with glutaraldehyde 2% (v/v) in a 1,4-piperazine-bis-(acid 2-ethanesulfonic) (Pipes) buffer (pH 7.4), at 4°C for 16 h. Dehydration was achieved by successive immersion in aqueous ethanol solutions of increasing concentration (30–100% v/v), ethanol–acetone solutions of increasing concentration (30–100% v/v), and finally in a critical point device (Baltec CPD 030) using CO_2 as transition agent (3 periods of 10 min, 40 °C, 80 atm). Afterwards the sample cuts were fixed on steel supports with charcoal glue and coated with gold using a JEOL metalizer (FFC-1100) at 1,100–1,200 V, 5 mA for 10 min. Samples were observed in a scanning electron microscope (Hitachi, S4100) at 20 kV.

At least ten images from independent samples were used for microstructural analyses and measurements. For a predefined area of the microphotographs, cell density was determined. Also, cell and intercellular space dimensions were determined using the UTHSCSA ImageTool Software (3.0).

Instrumental texture analysis

Texture profile analysis (TPA) was carried out by two compression cycles between parallel plates performed on cylindrical samples (diameter 8 mm, height 6 mm), at 20% strain, using a flat 75-mm diameter aluminium plunger (SMS P/75), with a 5-s set period of time between cycles.

Texture profile parameters were obtained from the force–time curves, according to the definitions of Szczesniak [23] and Bourne [24]. In this work a more fundamental approach was used by calculating stress and strain data, instead of the force/time/distance data typically used in TPA analysis. Briefly, *hardness* was defined as the peak stress during the first compression cycle (H), *cohesiveness* was defined as the ratio of the positive stress area during the second compression to that during the first compression (A2/A1), *springiness* was measured as the length of the downward compression during the second bite divided by the length of the downward compression during the first bite (d2/d1), and *chewiness* was quantified as the product of (hardness × cohesiveness × springiness). In addition, *adhesiveness* was defined as the negative area obtained during the first bite (upstroke curve, A3) and *resilience* was quantified as the area under the upstroke curve divided by the area under the downstroke curve, during the first bite (A4/A1).

In TPA measurements the samples were prepared with a radial orientation. From each radial cylinder of parenchyma tissue, cut equatorially from the surface to the core, one sample was produced.

Puncture tests were also performed using a 2-mm diameter cylindrical stainless steel probe, on whole pear samples, with a penetration depth of 2 mm, in order to obtain mechanical information at higher deformation levels. *Fracturability* was taken as the force at the first major drop in force curve and *firmness* was defined as the peak maximum force obtained during the puncture tests. The work done on the sample during the downstroke puncture was also measured.

Sampling for mechanical analysis was carried out through random samples of six different fruits. All mechanical tests were performed using a TA-Hdi Texture Analyser (Stable Micro Systems, Godalming, UK) equipped with a 5-kg load cell, at 0.5 mm/s compression rate.

Statistical analysis

Statistical analyses were performed using a one-way ANOVA (Sigmastat for Windows ver. 3.1, SPSS, USA) to analyse possible differences among average values for both, the results of image analyses of the microscopic observations and texture parameters. A multiple comparison Tukey test was applied to determine which groups were different, taking $p = 0.05$.

Results and discussion

Microstructural analysis of fresh and sun-dried pears

Histological analyses of transversal sections of fresh pear showed typical parenchyma cells. These cells are perfectly turgid with very few intercellular spaces, varying between isodiametric and egg-shaped form (Fig. 1). Cortical parenchyma cells showed average dimensions of 190 ± 40 μm (long axis) and 140 ± 60 μm (short axis), while those from zones/layers near epidermis showed slightly lower dimensions, 150 ± 50 μm (long axis) and 130 ± 40 μm (short axis) (Table 1). Despite these differences in parenchyma cell's dimensions, the volume of intercellular space remains approximately the same at 12% along the pear mesocarp. Similar differences on cell dimensions as a function of mesocarp location, with most compact cells near external sections, have been described for Blanquilla pear [25] and for olive [26]. Also, average cell dimensions are in conformity with the values presented for Blanquilla pear [25]. Sclereid clusters are also observed distributed in the parenchyma tissue, surrounded by parenchyma egg-shaped cells, with dimensions of 40 μm in the periphery of the fruit and 55 μm in the most internal areas, and an average density of 2.3 sclereid clusters per mm^2 (Table 1). The dimension of the sclereids (320 ± 50 μm) is in accordance with those reported for Blanquilla pear [25] and their average density agrees with the values reported for olive (0.5–3.8 sclereids mm^2) [26]. In S. Bartolomeu pears there are no significant differences in density of sclereid clusters (Table 1), contrary to what was described for Blanquilla pear [25], where

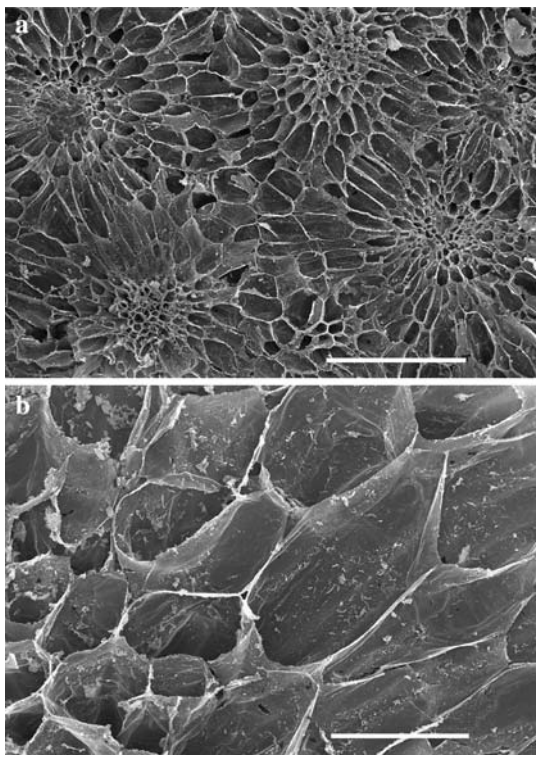

Fig. 1 Microphotographs of transversal sections of fresh S. Bartolomeu pear, obtained by SEM: **a** sclereid cluster surrounded by parenchyma cells with egg shape (*bar* 600 μm); **b** parenchyma cells of the cortical layer (*bar* 150 μm)

Table 1 Histological characteristics of both fresh and dry pear

	Fresh	Dry
Sub-epidermical layers		
Parenchyma cells		
Dimensions (μm)		
Long axis	150 ± 50^a	210 ± 40^a
Short axis	130 ± 40^a	50 ± 20^b
Intercellular space (% area)	12 ± 5^a	28 ± 10^b
Aggregate of sclereid clusters		
Density (no/mm^2)	2.3 ± 1.4^a	2.1 ± 0.6^a
Dimension (μm)	280 ± 70^a	220 ± 40^a
Average of sclereid clusters/aggregate	9 ± 4^a	11 ± 5^a
Average size of sclereid clusters	40 ± 15^a	35 ± 10^a
Intercellular space (% area)	3 ± 2^a	5.5 ± 3^a
Cell wall (% area)	92 ± 4.5^a	96 ± 2.7^a
Cortical layers		
Parenchyma cells		
Dimensions (μm)		
Long axis	190 ± 40^a	210 ± 30^a
Short axis	140 ± 60^a	50 ± 20^b
Intercellular space (% area)	11 ± 4^a	31 ± 12^b
Aggregate of sclereid clusters		
Density (no./mm^2)	2.5 ± 1^a	2.0 ± 1^a
Dimension (μm)	320 ± 50^a	290 ± 40^a
Average of sclereid clusters/aggregate	14 ± 8^a	10 ± 6^a
Average size of sclereid clusters	55 ± 20^a	60 ± 15^a
Intercellular space (% area)	3.0 ± 1.8^a	3.2 ± 1.0^a
Cell wall (% area)	92 ± 3^a	95 ± 4^a

For each row, means with the same superscript letter are not significantly ($p > 0.05$) different ($n = 10$)

sclereid clusters were more abundant on epidermal regions. Even though the percentage of cell wall area of sclereid clusters increases from 92 to 96% in sun-dried pear (Table 1), this difference was not statistically significant. Despite the unclear functions attributed to sclereid clusters, they appear to have an important role in the integrity maintenance and textural characteristics of tissues composed by parenchyma cells.

In sun-dried pears (Fig. 2) the turgor loss of parenchyma cells, showing signs of degradation and shape alteration is clear. In fresh pear tissues the intercellular spaces are mainly generated by the conjunction of three or four cells (Fig. 1b) and are much smaller than those observed in the sun-dried pear tissues (Fig. 2b). According to Table 1, the percentage of area occupied by the intercellular space in processed parenchyma tissues (11–12%) is 2–3 times higher than in fresh parenchyma tissues (28–31%). Many cells present fractured walls and no protoplast, leading to tissues with quite different aspect from those in fresh pear

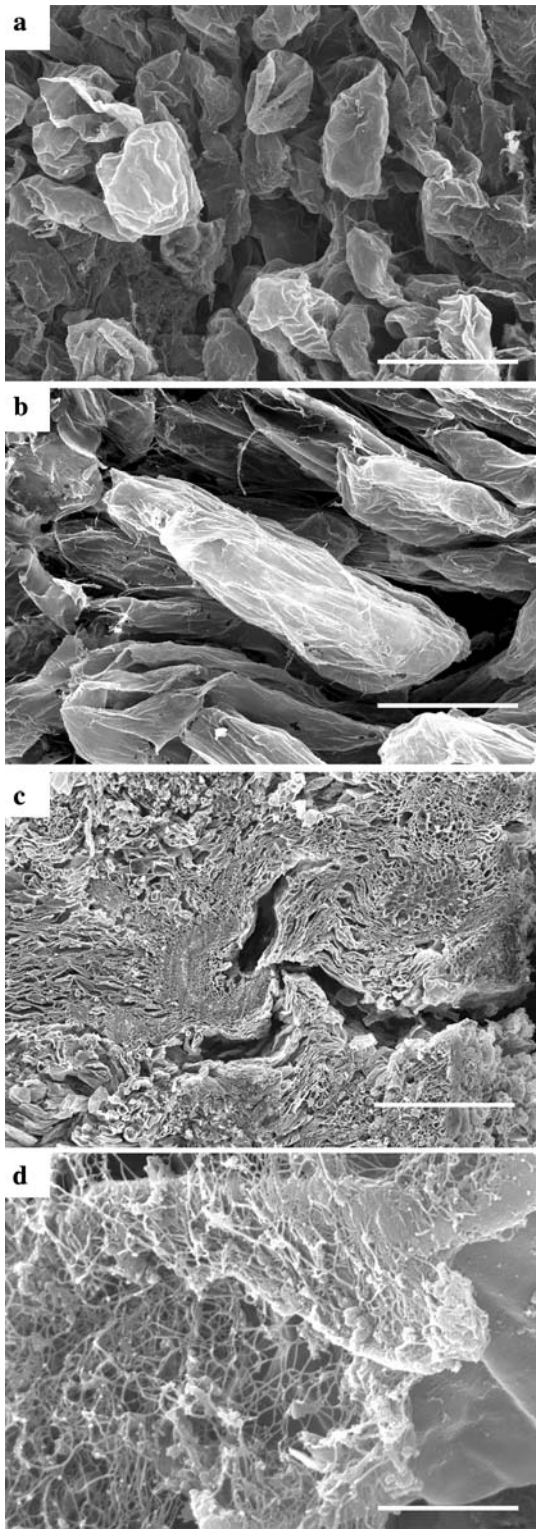

Fig. 2 Microphotographs of transversal sections of sun-dried S. Bartolomeu pear, obtained by SEM: **a** parenchyma cells that lost intercellular adhesion (*bar* 150 μm); **b** parenchyma cells without cellular adhesion, showing large intercellular spaces (*bar* 75 μm); **c** vascular lignified fractured bundle structures (*bar* 750 μm); **d** parenchyma cell with high cell wall degradation, showing tubular structures (*bar* 3 μm)

(Fig. 1). These differences are due to a more accentuated flattening of parenchyma cells, leading to reductions up to 60% in length of short axis, increasing the long axis from 150 to 210 μm in the cells of sub-epidermal layers and from 190 to 210 μm in the cells of cortical layers (Table 1). This flattening of the parenchyma cells, more pronounced in the external layers than in the internal ones, can be due to the compression conferred to the fruit tissue during processing.

Sun-dried pear cells show themselves to be more irregular in contours of the wall. Cell walls with irregular shape were also observed in fruits that suffered loss of tissue firmness due to ripening [10].

Comparing Figs. 1 and 2, it is obvious that there is a loss of adhesion between adjacent parenchyma cells in sun-dried fruits. Loss of cell adhesion has been explained by alterations in pectic polysaccharides of middle lamella [27, 28], namely by their solubilisation and degradation [10, 13, 26]. In ripening studies with numerous fruits a correlation was demonstrated between increasing of cell wall thickness, firmness loss and pectin solubilisation [10]. More regular cell walls and higher firmness were also attributed to a high concentration of neutral sugars [29].

No signs of degradation were detected in the thick secondary cell walls of the sclereid cells of sun-dried pear (results not shown). Sun-drying tissues also presented big fractures in the vascular lignified bundle structures (Fig. 2c), suggesting a strong tension, possibly due to the compression of the tissue during the processing.

In some regions of sun-dried pear thin long structures were also observed, possibly cellulose microfibrils (Fig. 2d), indicating the degradation of primary cell wall and probable decrease in cellulose content, as reported to occur during the ripening of olive tissues [13]. Microstructural studies of avocado ripening evidenced that the Cx-cellulase acts on the peripheric and non-cristaline cellulose microfibrils resulting in loss of cohesiveness of the fibril structure and changes in the linkages of the polysaccharides that constitute the matrix [30]. The increase of Cx-cellulase activity was also detected during the ripening of Rehder pear [31] and correlated with the decrease of cellulose content in an advanced stage of ripening of the fruit [32].

Texture analysis of fresh and sun-dried pears

Figure 3 illustrates representative TPA curves obtained for fresh and sun-dried pears. The higher hardness (maximum stress) and higher rigidity (initial slope) of the fresh pear specimens are clearly evident. For the fresh pear, the differences between the area and the width of each bite are also higher indicating lower cohesiveness and lower springiness.

Table 2 shows the texture parameters calculated from the compression TPA curves. For fresh fruits, hardness had a mean of 0.31 MPa, about 2× higher than the mean value

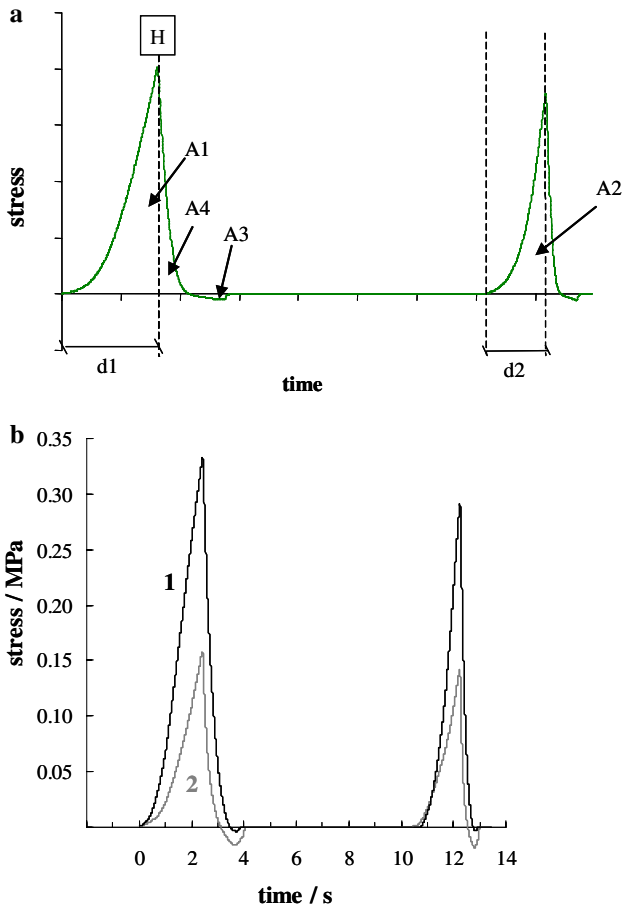

Fig. 3 TPA curves of fresh and sun-dried pear tissues. **a** Representative compression parameters shown by TPA curves; *H* maximum stress applied in the first cycle; *A* total area defined by a curve; *d* time/distance of the probe in each cycle until reaching the maximum force; **b** representative curves for fresh (*1*) and sun-dried (*2*) pears

obtained for the sun-dried pears. It means that for the first bite, the fresh pears would require more energy than the sun-dried samples, signifying that pears soften with the sun-drying treatment. Similar trend was observed for the second bite, except that lower energy would be spent in biting the food sample (Fig. 3). This result is expected providing that the drying process causes a loss of turgor pressure of parenchyma cells and a loss of cell adhesion, as observed by SEM (Figs. 1, 2).

On the other hand, sun-drying leads to a slight but consistent increase in the cohesiveness of the pear flesh. This textural attribute is related to the strength of the internal bonds making up the body of the sample. However, it is also a relative parameter strongly related to how the first bite affects the internal structure of the material. Sun-drying, being essentially a slow-drying process, is expected to result in uniform and dense products, where intercellular adhesion is much reduced. Contrarily, the raw plant tissue is notch-sensitive, and it can be represented by a strong

Table 2 Comparison between texture attributes obtained for fresh and sun-dried flesh pears measured by TPA compression tests

Sample	Fresh	Sun-dried
Hardness (MPa)	0.314 ± 0.016	0.163 ± 0.057
Cohesiveness (–)	0.54 ± 0.05	0.72 ± 0.02
Springiness (–)	0.72 ± 0.05	0.81 ± 0.08
Chewiness (MPa)	0.109 ± 0.018[a]	0.107 ± 0.059[a]
Resilience (–)	0.37 ± 0.05	0.29 ± 0.04
Adhesiveness (kPa s)	0.76 ± 0.44	7.52 ± 3.6

Mean ± standard deviation. Within columns, means with the same superscript letter are not significantly ($p > 0.05$) different

continuous matrix, the middle lamella, where the relatively weak cells are embedded. This kind of microstructure would be much more sensitive to the first bite, which is also correlated to the observed higher fracturability. The microstructural changes observed in the sun-dried pear flesh would weaken the matrix and lead to notch-insensitivity, and thus to a higher capacity to absorb energy with less structural damage, i.e. to a higher apparent cohesiveness.

Adhesiveness was also higher for the sun-dried pears than it was for fresh samples (Table 2). This result indicates that more work is necessary to overcome the attractive forces between the surface of the food and the surface of the other material with which the fruit comes into contact. Loss of water and concentration of the pear components may have contributed to the sticky characteristics of the sun-dried pears.

Springiness, which is a measure of the recovery in height after the sample has been compressed by the teeth during mastication, was higher for the sun-dried samples; the differences were low although statistically significant. The higher propensity of the dried pear flesh to return to their original shape after deformation indicates a rubbery behaviour. A different behaviour was observed for resilience, which means an "instant springiness", since this attribute is measured on the withdrawal of the first penetration, before the waiting period is started. Therefore, the dried tissue behaves like a material with elevated capacity to absorb energy, when elastically deformed, but showing higher apparent relaxation times, when compared to the fresh pear tissue.

In the low-deformation TPA compression conditions no distinguishing differences were observed between chewiness of fresh and dried tissue.

The above observations suggest that although fresh pears may require more mastication energy in the mouth for the first and second bites than sun-dried pears and their internal structure is more affected during the first bite, they may not spring back as much as the dried samples. The balance among opposite effects is responsible for the non-significant differences ($p > 0.05$) for chewiness.

Representative force/distance curves obtained from puncture tests are shown in Fig. 4. The puncture test involves essentially two components: a compression proportional to the area of the punch and shearing around the edge of the punch, which is proportional to the perimeter [33]. This type of test implies larger strains than the ones experimented by the sample under compression, which are well beyond the linear elastic range. During the compression TPA tests the degree of compression of 20% did not cause the rupture of the pear samples. Contrarily, the puncture tests lead to tissue rupture and involved more complex stress/strain profiles, precluding any fundamental correlation with the low strain compression TPA data. Anyway, puncture tests may provide useful complementary information at higher strains and are likely a better simulation of the mechanical process of mastication.

The puncture results obtained also support those obtained by TPA. The fresh pear is characterised by higher rigidity (very steep initial slope) and higher firmness and fracturability (Table 3). Contrarily, the dried pear deforms easily (low initial slope) and it does not show fracturability under the tested conditions. The dried pear can withstand higher energy before rupture occurs, but higher work is needed to be applied to the fresh pear in order to attain a given penetration degree (deformation).

It is well accepted that [34] the major modes of failure in fruit and vegetable tissues are cell rupture and cell debonding. Cell wall elasticity and firmness and intercellular adhesion are strongly dependent on the pectic substances of the middle lamella [7], and the observed histological modifications caused by drying are likely related to the previously observed changes on the polysaccharide components [15].

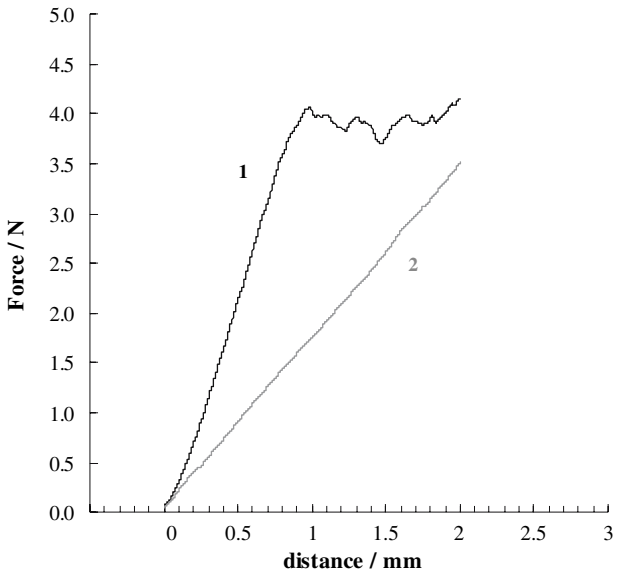

Fig. 4 Representative puncture curves for fresh (*1*) and sun-dried (*2*) pears

Table 3 Textural data obtained from one puncture cycle for fresh and sun-dried flesh pears

Sample	Fresh	Sun-dried
Fracturability (N)	3.8 ± 0.5	–
Firmness (N)	4.2 ± 0.5	3.5 ± 0.4
Work (J x 10^3)	20.0 ± 3.4	11.6 ± 1.4

Mean ± standard deviation. All means are significantly ($p < 0.05$) different

The texture of the fresh pear flesh reflects essentially a unified matrix comprising well-packed cells bonding together by strong intercellular adhesion. In the sun-dried pear flesh the observed cell wall degradation contributes to low rigidity of individual cells. In addition, the extent and strength of cellular adhesion is reduced and the intercellular spaces are increased, thus originating softer tissues whereas allowing higher stresses to be accommodated without exhibiting high structural damage and fracture during mechanical solicitation. The texture of these tissues is mainly related to a soft solid consisting of many individual cells. The easier cell separation would have now a more important role in the texture profile.

The higher rigidity, firmness and deformation work exhibited by the fresh pears under puncture tests also support the argument above that more energy would be required for cell-to-cell debonding in the raw pear parenchyma. In this case, the tissue fracture involves more rupture across the cell walls than would be expected for the sun-dried parenchyma.

Conclusion

Scanning electron microscopy and instrumental texture analysis were successfully applied to relate microstructure and texture of fresh and sun-dried pears. Both puncture and TPA compression tests showed tissue softening induced by drying processing. The decline in the hardness to about half of the initial value and the rise in the adhesiveness by about ten times of the sun-dried pears were the sharper textural changes observed. A slight increase in cohesiveness and springiness was also detected for the dried products, all together contributing to the peculiar texture properties of the S. Bartolomeu sun-dried pears.

The texture of the fresh pear flesh reflects essentially a unified matrix comprising well-packed cells strongly bonded together whereas the sun-dried pear flesh has softer tissues with a rubber texture. This resembles the behaviour of a soft solid with many individual cells distributed in a soft matrix, which explains its chewy texture.

These textural changes are related to important microstructural alterations in pear flesh induced by the loss of water, and probably other fruit components during sun-drying process, with emphasis on parenchyma cell shrinkage, cell separation, and damage of cell walls.

This study allowed us to understand the structural differences between sun-dried and fresh pear, permitting to infer about the related textural changes. This knowledge can be used to improve process control and end product quality.

References

1. Esper A, Muhlbauer W (1998) Renewable Energy 15:95–100
2. Ratti C, Mujumdar AS (2005) Drying of fruits. In: Barrett DM, Somogyi L, Ramaswamy H (eds) Processing fruits: science and technology, 4th edn. CRC Press, Boca Raton, pp 185–220
3. Barroca MJ, Guine RPF, Pinto A, Goncalves FM, Ferreira DMS (2006) Food Bioprod Process 84:109–113
4. Brett CT, Waldron KW (1996) Physiology and biochemistry of plant cell walls, 2nd ed. Chapman & Hall, Cambridge
5. Hills BP, Remigereau B (1997) Int J Food Sci Techn 32:51–61
6. Aguilera JM, Stanley DW (1999) Microstructural principles of food processing and engineering. Aspen Publishers, Gaithersburg
7. Waldron KW, Smith AC, Parr AJ, Ng A, Parker ML (1997) Trends Food Sci Technol 8:213–221
8. Lopes da Silva JA, Rao MA (1999) Role of rheological behavior in sensory assessment of fluid foods. In: Rao MA (ed) Rheology of fluid and semisolid foods. Aspen Publishers, Gaithersburg, pp 369–384
9. Coimbra MA, Waldron KW, Delgadillo I, Selvendran RR (1996) J Agric Food Chem 44:2394–2401
10. Redgwell RJ, MacRae E, Hallet I, Fischer M, Perry J, Harker R (1997) Planta 203:162–173
11. Stolle-Smits T, Beekhuizen JG, Recourt K, Voragen AGJ, Dijk CD (1997) J Agric Food Chem 45:4790–4799
12. Marsilio V, Lanza B, Campestre C, De Angelis M (2000) J Sci Food Agric 80:1271–1276
13. Mafra I, Lanza B, Marsilio V, Campestre C, De Angelis M, Coimbra MA (2001) Physiol Plant 111:439–447
14. Mafra I, Barros AS, Coimbra MA (2006) Carbohydr Polym 65:1–8
15. Ferreira D, Barros A, Coimbra MA, Delgadillo I (2001) Carbohydr Polym 45:175–182
16. Femenia A, Sánchez ES, Simal S, Rosselló C (1998) J Agric Food Chem 46:271–276
17. Asgar MA, Yamauchi R, Kato K (2004) Food Chem 87:247–251
18. Ferreira D, Guyot S, Marnet N, Delgadillo I, Renard CMGC, Coimbra MA (2002) J Agric Food Chem 50:4537–4544
19. Khan AA, Vincent JFV (1990) J Sci Food Agric 52:455–466
20. Ramana SV, Stengel E, Wolf W, Spiess WEL (1997) J Sci Food Agric 74:340–346
21. Alvarez MD, Saunders DEJ, Vincent JFV (2000) Eur Food Res Technol 210:331–339
22. Pinto G, Valentim H, Costa A, Castro S, Santos C (2002) In Vitro Cell Dev Biol-Plant 38:569–572
23. Szczesniak AS (1963) J Food Sci 28:410–420
24. Bourne MC (1978) Food Technol 32:62–66,72
25. Martin-Cabrejas MA, Waldron KW, Selvendran RR, Parker ML, Moates GK (1994) Physiol Plant 91:671–679
26. Marsilio V, Lanza B, De Angelis M (1996) J Sci Food Agric 70:35–43
27. Orfila C, Seymour GB, Willats WGT, Huxham IM, Jarvis MC, Dover CJ, Thompson AJ, Knox JP (2001) Plant Physiol 126:210–211
28. Atkinson RG, Schröder R, Hallett IC, Cohen D, MacRae EA (2002) Plant Physiol 129:122–133

29. Batisse C, Buret M, Coulomb PJ (1996) J Agric Food Chem 44:453–457
30. O'Donoghue EM, Huber DJ, Timpa JD, Erdos GW, Brecht JK (1994) Planta 194:573–584
31. Yamaki S, Kakiuchi N (1979) Plant Cell Physiol 20:301–309
32. Yamaki S, Machida Y, Kakiuchi N (1979) Plant Cell Physiol 20:311–321
33. Bourne MC (2002) Food texture and viscosity, 2nd edn. Academic, New York
34. Pitt RE (1992) Viscoelastic properties of fruits and vegetables. In: Rao MA, Steffe JF (eds) Viscoelastic properties of foods. Elsevier Applied Science, New York, pp 49–76